Chapter 7

Characterising the spatial distribution of transmissivity in the mountainous region: Results from watersheds in central Taiwan

Po-Yi Chou, Jung-Jun Lin, Shih-Meng Hsu, Hung-Chieh Lo, Po-Jui Chen, Chien-Chung Ke, Wong-Ru Lee, Chun-Chieh Huang, Nai-Chin Chen, Hui-Yu Wen & Feng-Mei Lee

Geotechnical Engineering Research Center, Sinotech Engineering Consultants Inc., Taipei, Taiwan

ABSTRACT

Complex geological features are present in the mountainous regions of Taiwan. Strongly folded, faulted and highly fractured formations are common, the delineation of groundwater producing zones is, therefore, challenging. However, progress towards characterising the transmissivity in the mountainous region of Taiwan has been made. There are three major watersheds: the Dajia, Wu and Jhuoshuei River. A total of 65 boreholes have been drilled, various types of well logging, rock core inspection and packer tests carried out. Using these data gathered during the past three years, a conceptual model has been developed which delineates the spatial distribution of hydraulically transmissive conduits in the region.

7.1 INTRODUCTION

Groundwater plays a pivotal role in sustainable development. In Taiwan, a great number of studies have been devoted to investigating the groundwater system in the alluvial plains (Hsu, 1998; Ting *et al.*, 1998; Jang & Liu, 2004; Chen *et al.*, 2005; Chou & Ting, 2007; Tu *et al.*, 2011). In total, nine critical groundwater basins have been recognised on the basis of their water production capabilities as well as local water demand. However, along with the ever-growing population and the rising demand for water, recent studies have also shown that the majority of these alluvial groundwater basins are under stress. Interest has been raised over whether the productivity of upstream hard-rock aquifers could provide and meet the needs of downstream water users. Yet, this is a difficult and challenging task as previous studies (Maréchal *et al.*, 2004; Foster, 2012) indicate that groundwater bodies are not universally distributed within hard-rock formations.

The mountainous regions have greater changes in elevation, slope gradient, geological structure and stratigraphic composition than the alluvial areas. The spatial variability and uncertainty of aquifer hydraulic parameters in mountainous regions is higher, and this is one of the main difficulties in modelling such terrain. The earlier investigations concentrated on the alluvium and there remain many gaps in the spatial distribution of transmissivity in the mountainous region. As a result, insufficient base-line data are available to enable reliable analysis and accurate prediction with which to inform policy makers.

Under the co-ordination of the Central Geological Survey (CGS) of Taiwan, a nationally-funded investigation programme was launched in 2010 to improve the understanding of the groundwater resources in the mountainous region. Exploratory drilling and related studies are being carried out by Sinotech Engineering Consultants for, and in collaboration with two technical institutions. The particular aims are (1) to obtain the depth-distribution of geological attributes and geophysical parameters, and (2) to assess the hydrogeological character of the upstream bedrock aquifers. The first phase of the programme (2010–2013) focussed on central Taiwan, which is home to nearly 1 in 4 (5.6 million) of the population of Taiwan. The investigation has been carried out in three major watersheds, including Dajia, Wu and Jhuoshuei River. This chapter provides a brief description of the study area, the methods of interpretation, and the investigation results to date.

7.2 THE STUDY AREA

The study area (Figure 7.1) is situated roughly at latitude and longitude of 24°00'N and 121°00'E and covers an area of 6560square kilometres. The Central Mountain Range (3930 m a.s.l.) runs from north to south and forms the major watershed divide in Taiwan. The catchment watersheds between the Dajia, Wu and Jhuoshuei River are oriented east west with the rivers draining towards the Taiwan Strait. The geographical setting of the study area can be split conceptually into two sub-regions according to the lithological features. Bordering the Central Mountain Range, region one is located in the east of the study area. In this region, the topographic slopes are steep and rugged. The predominant lithologies (ranging from Eocene to Early Miocene) are mainly composed of highly metamorphic argillite, slate and phyllite. Region two is located in the west and is underlain by Miocene to Pleistocene sedimentary rocks. A series of east west fold-and-thrust belts is present in the region. The predominant lithology is massive sedimentary sandstone, siltstone and shale. An apparent lithological transition zone can be recognised in the middle of the area, in which the upper part is composed mainly of hard shale, whereas the lower part is composed of coarse quartz sandstone.

The surficial material comprises unconsolidated weathering materials, *i.e.* the regolith layers, which consist of soil, infills, alluvium, colluvium, and saprolite. The average thickness is 17.5 m. Twenty hydrogeologic units have been recognised based on the age and the rock type, and seventeen of them have been examined over the last three years. The characterisation of these hydrogeologic units is summarised in Table 7.1.

A preliminary map of groundwater potential zones has been prepared to help determine optimum drilling sites. During 2010 to 2012, 65 exploratory boreholes have been drilled to a depth of 100 m, 15 in the Dajia River basin, 16 in the Wu River basin and 34 in the Jhuoshuei River basin using a combination of mechanical and pneumatic drilling rigs. Rock samples are recovered for the initial lithostratigraphic

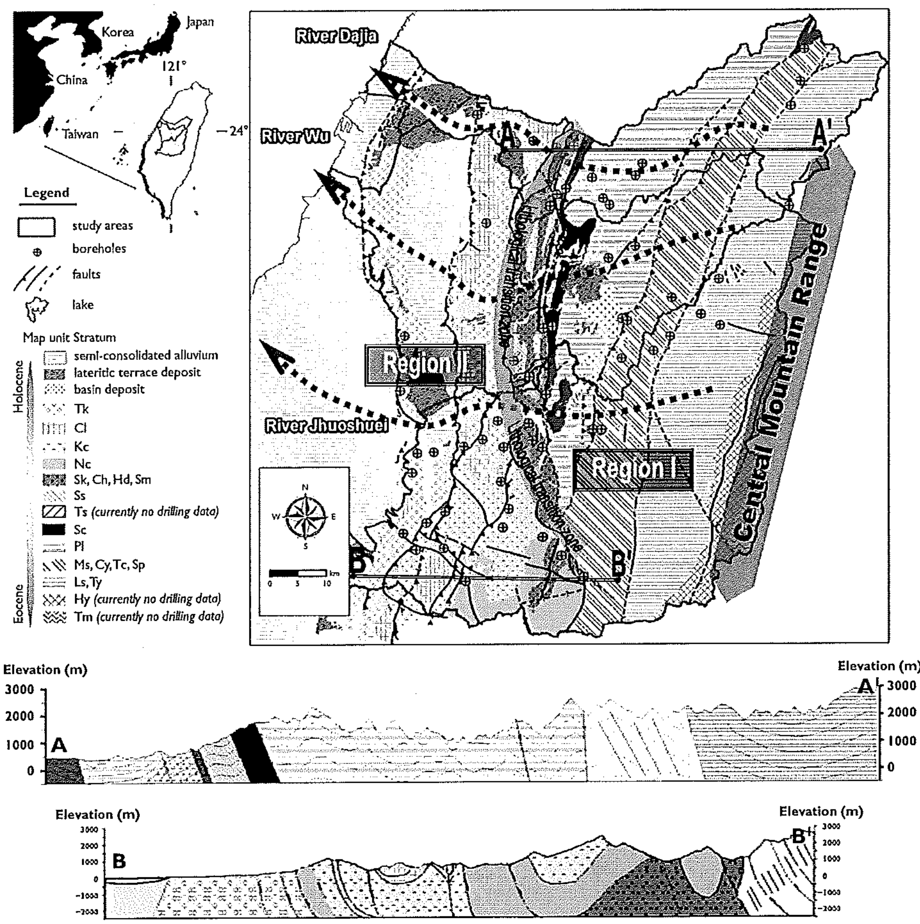

Figure 7.1 Geological setting (up) and two geological cross sections (east-west) (down) of the study area. (*See colour plate section, Plate* 22).

identification and subsequent laboratory analysis. A variety of geophysical logs and flow measurements were carried out.

7.3 FIELD INVESTIGATIONS

The general procedure of field investigations is shown in Figure 7.2. Comparing the driller's log and the geologists' report, a general characterisation can be made for each site of the distribution of fractures and the corresponding permeability of the rock mass. This indicates the depths to which water-bearing fractures are presented, but also any formation breaks within zones of no core recovery. This is as an essential procedure prior to geophysical logging. A number of borehole logging tools are used and aquifer hydraulic testing is carried out in each borehole.

Table 7.1 Geologic formation of hydrogeologic units in the study area.

Geologic formation (code)	*Geological epoch*	*River Basin*	*Rock type*	*Number of boreholes*
TouKeshan formation (Tk)	Pleistocene	J	S	6
ChoLan formation (Cl)	Pleistocene ~ Pliocene	D, J, W	S	4
KueiChulin formation (Kc)	Pliocene ~ Miocene	D, J	S	7
NanChuang formation (Nc)	Miocene	J, W	S	2
ShenKeng formation (Sk)	Miocene	J, W	S	6
ChangHukeng formation (Ch)	Miocene	J	S	2
ShihSzeku formation (Ss)	Miocene	D, W	S	2
Shihman formation (Sm)	Miocene	D, W	S	2
HouDongkeng (Hd)	Miocene	D, W	S	2
LuShan formaiton (Ls)	Miocene	J, W	M	4
TaYuling formation (Ty)	Miocene	J	M	1
ShuiChanglium formation (Sc)	Oligocene	D, J, W	M	3
MeiShi formation (Ms)	Oligocene	D	M	2
PaiLeng formation (Pl)	Oligocene ~ Eocene	D, J, W	M	12
TaChien formation (Tc)	Oligocene ~ Eocene	J, W	M	3
ChiaYang formation (Cy)	Oligocene ~ Eocene	D, J, W	M	3
ShihPachungchi formation (Sp)	Eocene	J, W	M	2

D: Dajia River basin; **J**: Jhuoshuei River basin; **W**: Wu River basin; **S**: Sedimentary rock; **M**: metamorphic rock

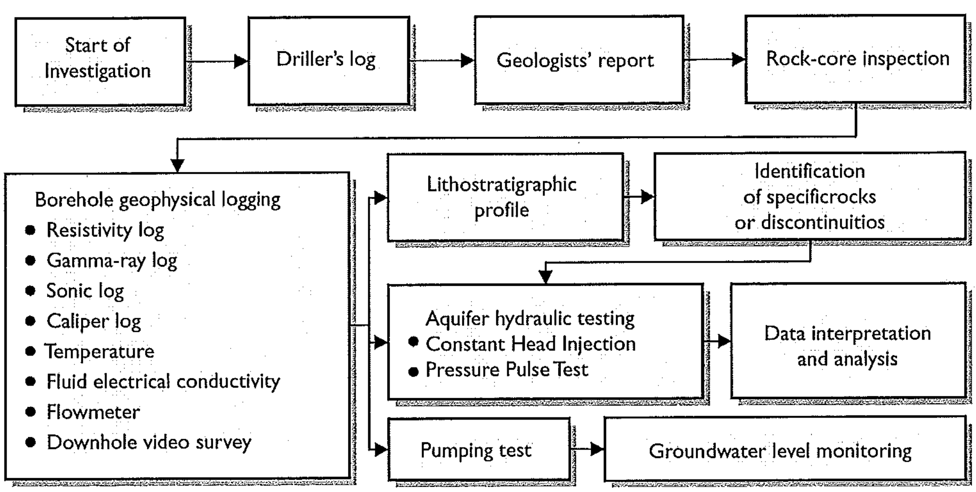

Figure 7.2 Flow-chart of investigation.

7.3.1 Borehole-geophysical logs

- The **Resistivity log** measures the resistance of the formation fluid to an induced electrical current, and is closely related to the total volume of interconnected pore spaces in the bedrock, namely the effective porosity that contributes to groundwater flow. The range is governed by the electrode spacing, and this is typically set at either 40.6 cm (short) or 162.6 cm (long).
- The **Gamma-ray log** is used for characterising the radioactivity emanating from the rock surrounding the borehole, and is primarily related to the rock type and the relative proportion of clay minerals in the formation. Generally, a lower gamma-ray response indicates the presence of a coarse-grained formation with a favourable water-transmitting capacity.
- The **Sonic log** measures the transmission of compressional waves through the formation, and is related to the rock strength, its elastic properties and porosity. The longer the travel time, or the slower the wave propagation velocity, the higher the porosity and water-transmitting capacity.
- The **Caliper log** provides a continuous profile of the borehole diameter with depth.
- The **Temperature** and **Fluid electrical conductivity logs** assist in identifying the presence of hydraulically active discontinuities.
- Two types of **Flowmeter** are used to delineate preferential flow paths and connetivity between fractures. The impeller flowmeter provides a continuous log of the general flow rate in the borehole, while the heat-pulse flowmeter can be used to further delineate the direction of flow.
- Lastly, the **downhole video survey** provides a clear visual inspection of the borehole walls. Not only can the geologists' report can be confirmed, but the dip-azimuth, aperture and infilling material can also be identified. The high resolution acoustic televiewer (HiRAT) and optical televiewer (OPTV) were used. The HiRAT can be carried out in a mud-filled borehole, while the OPTV is applicable in dry or clean water-filled holes.

Using all the geophysical data a total of 365 segments were identified for in-situ packer tests.

7.3.2 Aquifer hydraulic testing

The packer testing was carried out to determine the transmissivity of the rock mass and of individual fracture-zones that are presumed to be conductive. This standard and reliable procedure that has been applied since the 1950s and is widely employed in groundwater investigation (Mejías *et al.*, 2009; Chou *et al.*, 2012). The basic concept is to isolate a specific interval of the wellbore with inflatable packers, inject water to a set constant pressure, and measure the pressure change over time.

The packer assemblies include discrete rubber packers, pressure transducers, flow regulators, water pumps, nitrogen cylinder, and the hoisting system. All the equipment is calibrated in the laboratory and in the field. A double-packer system is used (Figure 7.3). The sealed-off interval is fixed at 1.5 m. Each test starts by applying the Constant Head Injection (CHI) test, which needs a volume of pressurised water to pass through the test section for a prolonged period of time. The testing procedures

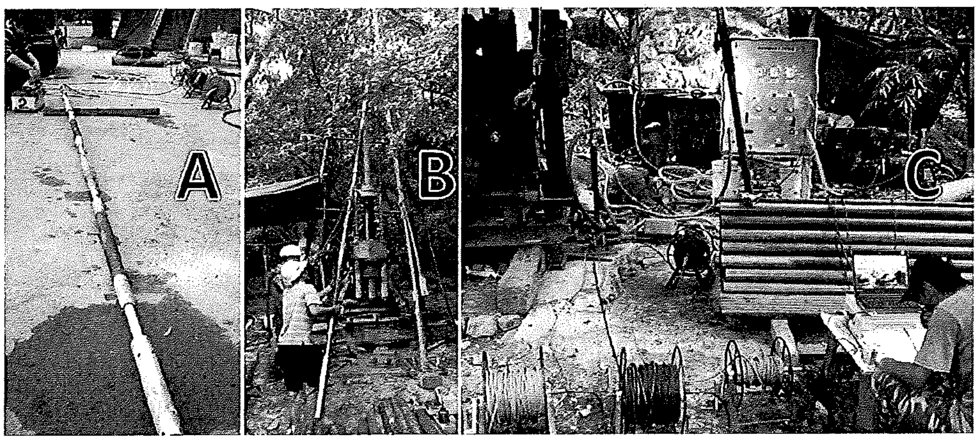

Figure 7.3 Photos taken during packer testing, (A) equipment calibration, (B) rig transfer, (C) 3ata recording and analysis. (*See colour plate section, Plate 23*).

followed the American Society for Testing and Materials (ASTM) methods. Water is injected with a constant pressure of 0.2 MPa in order to not damage to the aquifer. Each CHI test takes at least three hours including calibration (Figure 7.3A), rig transfer (Figure 7.3B), packer inflation, data recording (Figure 7.3C) and pressure recovery. In case no significant water flow rate can be measured, an alternative hydraulic test method, the Pressure Pulse (PP) test, can be applied, i.e. with extremely low transmissivity. A much longer period of testing time is usually needed. The variation of hydraulic head and injected flow rate within the test sections are recorded and stored in a data-logger.

Transmissivity is determined through the interpretation of the injected flow rate by means of the AQTESOLV analysis software. AQTESOLV offers a variety of analytical solutions, which enable both visual and automatic type curve matching of the test data. For all test segments that are capable of being tested by CHI test, the generalised radial flow (GRF) model (Barker, 1988) is applied. The GRF model accounts for the multi-scale fracture network heterogeneity (Le Borgne *et al.*, 2004). The conceptual aquifer geometry in a GRF model is assumed to be a fractal network of conduits, which matches the geological conditions in Central Taiwan. In addition, this model generalises the flow dimension to non-integral values. A coefficient 'n' is used, which denotes the flow dimension (the change of the cross-sectional area to the flow) according to the distance from the borehole (Walker and Roberts, 2003), and is set to be 1 for planar flow, 2 for cylindrical flow and 3 for spherical flow. The limitation of the GRF model is that it does not account for any inertial effect (Audouin & Bodin, 2008). The model is written as:

$$S_s \frac{\partial h}{\partial t} = \frac{K}{r^{n-1}} \frac{\partial}{\partial r}\left(r^{n-1} \frac{\partial h}{\partial r} \right) \qquad (1)$$

$$T = K \times 1.5^{(3-n)} \tag{2}$$

where S_s represents the specific storage of the aquifer [1/L]; $h(r, t)$ denotes the change in hydraulic head [L] with time, r represents the radial distance from the borehole [L]; K represents the hydraulic conductivity [L/T]; T represents the coefficient of transmissivity [L^2/T]; n denotes the flow dimension according to the distance from the borehole.

For those boreholes that are productive, pumping tests are carried out at the final stage for estimating long-term yield. During the test, water is extracted by using the submersible electric pump (MP1), and a constant pumping rate at a discharge of 70 l/min is maintained for 24 hours. By monitoring the drawdown in every 30 seconds, the transmissivity and storage coefficient of the aquifer are determined using AQTESOLV using the analytical solution of Moench (1997). As soon after the intrusive investigations and geophysical surveys are completed, two piezometers were installed at selected depths in each borehole for long-term groundwater level monitoring, one is for observing the groundwater level fluctuation in the regolith, and the other is for that in deep bedrock aquifers.

7.4 RESULTS

7.4.1 Interpretation of hydraulic tests: A statistical perspective

The focus for the packer tests was the 193 segments that were tested by the Constant Head Injection (CHI) method under a steady flow rate. These segments are the primary conductive zone compared to the less productive segments tested by the Pressure Pulse (PP) method. The estimated transmissivity values derived from CHI are plotted (Figure 7.4) on a logarithmic scale against the corresponding depth on a linear scale, with the majority (65%) of estimates lying between 0.1 and 10 m^2/day. A relatively high degree of uncertainty regarding the spatial variability of transmissivity is present. In order to characterise the core data and reduce bias caused by outliers, the geometric mean of the transmissivities across a 10-m depth interval is used, and a slight decrease in transmissivity with depth can be obtained. The higher transmissivities (0.54~0.95 m^2/d) were obtained above 30 m depth, and between 40 to 50 m depth (0.44 m^2/day). The lower depths (fractured bedrock) have transmissivity values in the range 0.22~0.28 m^2/day. A statistical summary of transmissivities is shown in Table 7.2.

Further qualitative characterisation can be made by classifying the magnitude of transmissivity as: (1) high-transmissive zones: $10 > T \geqq 1$ m^2/day, (2) medium-transmissive zones: $1 > T \geq 0.1$ m^2/day, (3) low-transmissive zones: $0.1 > T \geq 0.01$ m^2/day. It is apparent that several significantly high transmissive zones are present at depths between 30 to 60 m. and these may be the predominant pathway for groundwater flow. This suggests that assigning depth-dependent-transmissivity in multiple layers is not sensible within a conceptual hydrogeological model for the mountain region and that it is more appropriate to specify the representative transmissivity values (bounded by the arithmetic and the harmonic means) for different depth domains.

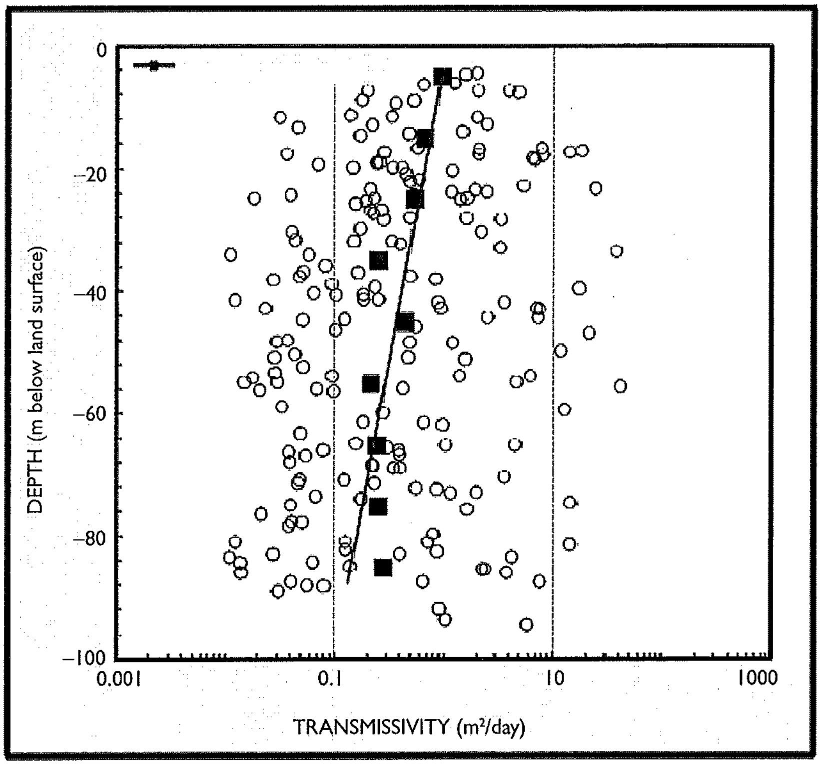

Figure 7.4 Estimated transmissivity derived from the CHI method against depth.

Table7.2 Statistical summary of transmissivities (m²/day) across a 10-m depth interval.

Depth (m)	*Geometric mean*	*Arithmetic mean*	*Standard deviation*	*Harmonic mean*
<10	0.95	1.57	1.53	0.55
10–20	0.66	2.64	4.47	0.19
20–30	0.54	1.90	4.84	0.18
30–40	0.25	3.16	8.97	0.07
40–50	0.44	2.74	5.04	0.09
50–60	0.22	3.30	9.22	0.05
60–70	0.24	0.55	1.02	0.13
70–80	0.25	1.35	3.28	0.08
80–90	0.28	1.74	3.23	0.05
Total	**0.37**	**2.18**	**5.38**	**0.09**
highest				
lowest				

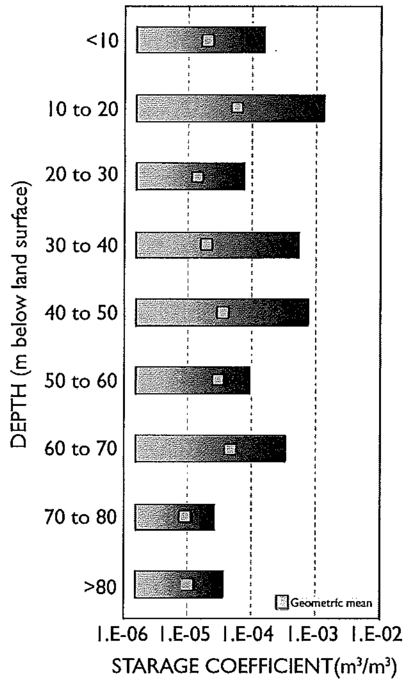

Figure 7.5 Estimated values of storage coefficient against depth.

The estimated distribution (1st–3rd quartile and geometric means) of storage coefficient for each depth interval is shown in Figure 7.5. The higher storage coefficients occur above a depth of 20 m, coinciding with the average thickness of regolith. This indicates that the transition zone between regolith and bedrock forms the upper productive water-bearing channel. The second high zone occurs at depths between 30 and 50 m. By comparing the arithmetic mean of transmissivity values (Table 7.2) for the same depth range, the second productive water-bearing layer is identified coinciding with dense fracture networks. In comparison with the first layer, this layer is a relatively narrow conduit for groundwater flow. According to the definition given by Lin (2010), both layers can be viewed as the Critical Zone (CZ), in which continuous exchange of water, energy and mass take place.

In the deeper zones the water storage capacity of the bedrock is limited. The slightly higher storage capacity layers are at depths from 60 to 70 m, but the corresponding transmissivity values are low. An explanation is that only a small portion of the open fractures above this depth range are hydraulically active, and the majority are sealed by quartz, calcite, chlorite, or filled with mud or clay. This is confirmed by the geophysical logs and rock core inspection.

A conceptual hydrogeologic model can be established, which provides a general but practical characterisation of groundwater flow in the mountain region. The water-bearing capacity of each horizon is shown in Figure 7.6 by different grey scales. The

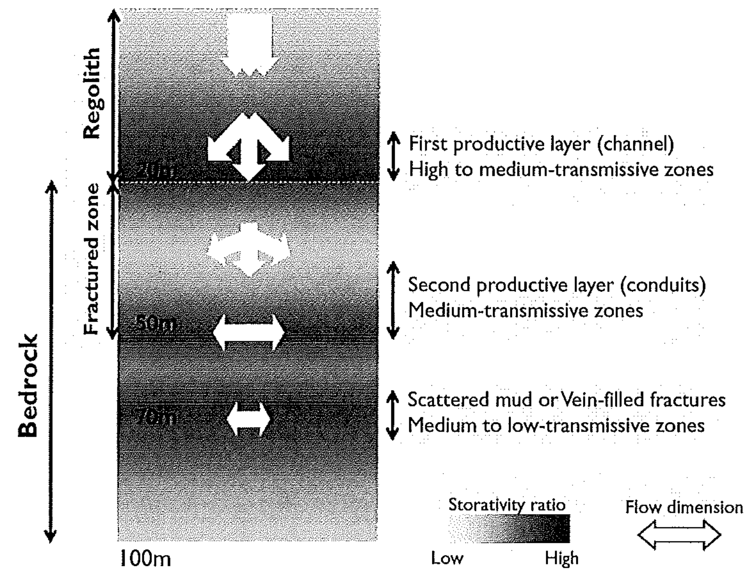

Figure 7.6 A conceptual hydrogeological model for groundwater flow in the mountainous region (not to scale).

darker-grey area corresponds to higher storativity ratio. The principal flow dimension in each horizon is also given, the longer arrow represents a potential for higher transmissivity values. There are two principal productive layers in this conceptual hydrogeologic model. The first is likely to appear at the transition zone from the regolith to bedrock. The second is the hydraulically active fractured zone within the uppermost portion of bedrock, which, as described by Sukhjia *et al.*, (2006), needs to connect to a distant recharge source beyond the edge of the overlying weathered zone. Dewandel *et al.*, (2006) have also illustrated that, in granite-type rocks, this layer may assume most of the transmissive capacity of the aquifer.

7.4.2 Vertical weathering profile in different geological formations: An integrated *view*

Certain zones within the regolith and the underlying bedrock have sufficient permeability to yield water to wells (Chilton & Foster, 1995). It is important to characterise the transmissivity at different zones. Generally, three distinct zones in terms of the degree of weathering can be identified above the bedrock: (1) the soil or infill deposits (R-s/b), (2) the highly weathered alluvium- or colluvium zone (R-a/c), and (3) the less weathered saprolite- or saprock zone (R-sl/sr). By integrating data obtained from drill core and aquifer hydraulic testing, the conceptual weathering profile of sedimentary and metamorphic formations (Figure 7.7), as well as the water-transmitting capacity of each weathering zones can be presented.

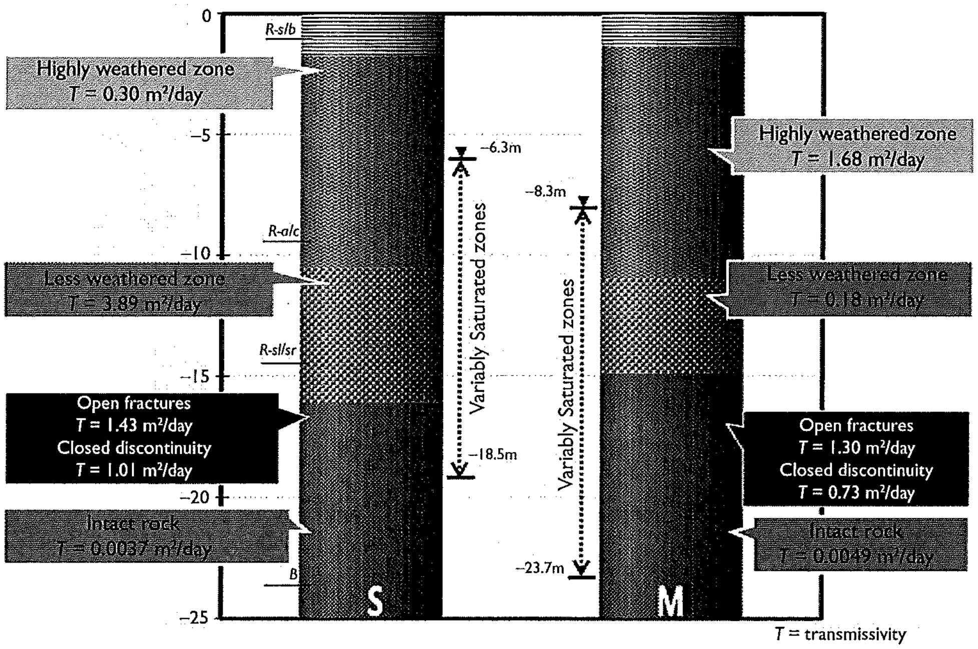

Figure 7.7 Vertical weathering profile in different lithologic settings (S for sedimentary, M for metamorphic rock).

Based on the data obtained from the HiRAT and OPTV, it is possible to distinguish the open fractures (with aperture ≥ 1 mm) from the closed ones (such as hairline cracks) within the bedrock. Therefore, the corresponding water-transmitting capacity possessed by the open fractures and the closed discontinuities is also presented in Figure 7.7. The open fractures identified in both types of formations are generally the high-transmissive zones; their water-transmitting capacities are 1.3~1.8 times greater than the estimates obtained from the closed discontinuities.

The zone of soil and backfill in the mountainous region is thin, generally less than 2 m, while the thickness of R-a/c zone and R-sl/sr zone are much greater. The arithmetic mean of transmissivities at each weathering zones suggests that in the sedimentary formations, the R-a/c zone possesses a lower transmissive capacity (T = 0.30 m^2/day) than the R-sl/sr zone (T = 3.89 m^2/day). The R-sl/sr zone is the first productive layer in the sedimentary formations (Figure 7.6), and the hydraulically active fractured zone in the uppermost portion of bedrock (T = 1.01~1.43 m^2/day) is the second one. Comparatively, in metamorphic formations, the R-a/c zone is found to have a higher transmission capacity (T = 1.68 m^2/day) than the R-sl/sr zone (T = 0.18 m^2/day). As such, the R-a/c zone ought to be the first productive layer in the fractured bedrock, while the second one is the hydraulically active fractured zone at the uppermost portion of bedrock (T = 0.73~1.30 m^2/day).

Since groundwater-level data are collected at each borehole, the relative groundwater elevations with respect to the weathering profile are also displayed in Figure 7.7.

In the sedimentary formations, the groundwater level lies approximately 6.3 to 18.5 m below ground level. In fractured bedrock, the groundwater level generally lies at deeper depths from 8.3 to 23.7 m. This shows the spatial variability of the vadose zone and the actual range of the Critical Zone in the two different settings. The thicker saturated weathered zone and its shallow water table offers a more favourable groundwater potential than fractured bedrock.

7.5 CONCLUSIONS

Interest in the yield of aquifers in the mountainous headwater basins is driven by increasing demand on the alluvial plains in Taiwan. It is difficult to assess the groundwater potential in such upland fractured bedrock and regolith terrain, which, as Klemeš (1988) argues, is the "blackest black box" in the hydrological cycle. Information from field investigations including lithostratigraphic identification, borehole-geophysical logs, aquifer hydraulic tests, enables a preliminary understanding of the distribution of storage and transmissivity in the Dajia, Wu and Jhuoshuei River catchments.

Two principal productive layers can be identified. The first is the transition zone between the regolith and the bedrock at a depth above 20 m, and the second is the hydraulically active fractured zone existing within the range from 30 to 50 m below the surface in the fractured bedrock. A conceptual hydrogeologic model is proposed that accounts for the spatial distribution of groundwater potential zones in this mountainous region. In the sedimentary formations and regolith, the higher transmissivity zone is found corresponding to the saprolite – or saprock, while in the metamorphic formations, the alluvium – or colluvium zone near the ground surface is possesses the best groundwater potential.

ACKNOWLEDGMENTS

The authors are grateful to our colleagues from the geotechnical testing group, Sinotech, in assisting the field work, and to the financial support of the Central Geological Survey, Ministry of Economic Affairs (MOEA) of Taiwan. We are also grateful to Prof. Dr. Stephen Foster and Irena Krusic-Hrustanpasic for their critical review and useful comments.

REFERENCES

Audouin O., Bodin J. (2008) Cross-borehole slug test analysis in a fractured limestone aquifer. *Journal of Hydrology* 348, 510–523.

Barker J.A. (1988) A generalised radial flow model for hydraulic tests in fractured rock. *Water Resources Research* 24, 1796–1804.

Chen J.F., Lee C.H., Yeh T.C., Yu J.L. (2005) A water budget model for the Yun-Lin Plain, Taiwan. *Water Resources Management* 19, 483–504.

Chilton P.J., Foster S.S.D. (1995) Hydrogeological characterization and water-supply potential of basement aquifers in Tropical Africa. *Hydrogeology Journal* 3, 36–49.

Chou P.Y., Lo H.C., Hsu S.M., Lin Y.T., Huang C.C. (2012) Prediction of hydraulically transmissive fractures using geological and geophysical attributes: a case history from the mid Jhuoshuei River basin, Taiwan. *Hydrogeology Journal* 20, 1101–1116.
Chou P.Y., Ting C.S. (2007) Feasible groundwater allocation scenarios for land subsidence area of Pingtung Plain, Taiwan. *Water Resources* 34, 259–267.
Dewandel B., Lachassagne P., Wyns R., Maréchal J.C., Krishnamurthy N.S. (2006) A generalised 3-D geological and hydrogeological conceptual model of granite aquifers controlled by single or multiphase weathering. *Journal of Hydrology* 330, 260–284.
Foster S., (2012) Hard-rock aquifers in tropical regions: using science to inform development and management policy. *Hydrogeology Journal* 20, 659–672.
Hsu S.K. (1998) Plan for a groundwater monitoring network in Taiwan. *Hydrogeology Journal* 6, 405–415.
Jang C.S., Liu C.W. (2004) Geostatistical analysis and conditional simulation for estimating the spatial variability of hydraulic conductivity in the Choushui River alluvial fan, Taiwan. *Hydrological Processes* 18, 1333–1350.
Klemeš V. (1988) Foreword. In: L. Molnâr L. (Eds.) *Hydrology of mountainous areas*. IAHS Publication No. 90.
Le Borgne T., Bour O., de Dreuzy J.R., Davy P., Touchard F. (2004) Equivalent mean flow models for fractured aquifers: Insights from a pumping tests scaling interpretation. *Water Resources Research* 40, XX-XX.
Lin H. (2010) Earth's Critical Zone and hydropedology: concepts, characteristics, and advances. Hydrology and Earth System Science 14, 25–45.
Maréchal J.C., Dewandel B., Subrahmanyam K. (2004) Use of hydraulic tests at different scales to characterize fracture network properties in the weathered-fractured layer of a hard rock aquifer, Water Resour Res 40, XX-XX.
Mejías M., Renard P., Glenz D. (2009) Hydraulic testing of low permeability formations: a case study in the granite of Cadalso de los Vidrios, Spain. *Engineering Geology* 107, 88–97.
Moench A.F. (1997) Flow to a well of finite diameter in a homogeneous, anisotropic water table aquifer. *Water Resource Research* 33, 1397–1407.
Sukhija B.S., Reddy D.V., Nagabhushanam P., Bhattacharya S.K., Jani R.A., Kumar D. (2005) Characterisation of recharge processes and groundwater flow mechanisms in weathered-fractured granites of Hyderabad (India) using isotopes. *Hydrogeology Journal* 14, 663–674.
Ting C.S., Zhou Y., de Vries J.J., Simmers I. (1998) Development of a preliminary ground water flow model for water resources management in the Pingtung Plain, Taiwan. *Ground Water* 35, 20–36.
Tu Y.C., Ting C.S., Tsai H.T., Chen J.W., Lee C.H. (2011) Dynamic analysis of the infiltration rate of artificial recharge of groundwater: a case study of Wanglong Lake, Pingtung, Taiwan. *Environmental Earth Science* 63, 77–85.
Walker D.D., Roberts R.M. (2003) Flow dimensions corresponding to hydrogeologic conditions. Water Resources Research 39: 1349–XX.